NASA's Surface Deformation and Change Mission Study

Stephen Horst
Jet Propulsion Laboratory
California Institute of Technology
4800 Oak Grove Dr.
Pasadena, CA 91107
Stephen.J.Horst@jpl.nasa.gov

Jonathan Chrone
NASA Langley Research Center
1 NASA Dr.
Hampton, VA 23666
Jonathan.D.Chrone@nasa.gov

Shaun Deacon
NASA Langley Research Center
1 NASA Dr.
Hampton, VA 23666
Shaun.A.Deacon@nasa.gov

Charles Le
Jet Propulsion Laboratory
California Institute of Technology
4800 Oak Grove Dr.
Pasadena, CA 91107
Charles.T-C.Le@jpl.nasa.gov

Adrien Maillard
Jet Propulsion Laboratory
California Institute of Technology
4800 Oak Grove Dr.
Pasadena, CA 91107
Adrian.Maillard@jpl.nasa.gov

Andrew Molthan
NASA Marshall Spaceflight Center
Martin Rd SW
Huntsville, AL 35808
Andrew.Molthan@nasa.gov

Anh Nguyen
NASA Ames Research Center
Freeman Ln
Mountain View, CA 94043
Anh.N.Nguyen@nasa.gov

Batuhan Osmanoglu
NASA Goddard Spaceflight Center
8800 Greenbelt Rd
Greenbelt, MD 20771
Batuhan.Osmanoglu@nasa.gov

Shadi Oveisgharan
Jet Propulsion Laboratory
California Institute of Technology
4800 Oak Grove Dr.
Pasadena, CA 91107
Shadi.Oveisgharan@jpl.nasa.gov

Martin Perrine
NASA Goddard Spaceflight Center
8800 Greenbelt Rd
Greenbelt, MD 20771
Martin.L.Perrine@nasa.gov

Rashmi Shah
Jet Propulsion Laboratory
California Institute of Technology
4800 Oak Grove Dr.
Pasadena, CA 91107
Rashmi.Shah@jpl.nasa.gov

Ekaterina Tymofyeyeva
Jet Propulsion Laboratory
California Institute of Technology
4800 Oak Grove Dr.
Pasadena, CA 91107
Katia.Tymofyeyeva@jpl.nasa.gov

Christopher Wells
Jet Propulsion Laboratory
California Institute of Technology
4800 Oak Grove Dr.
Pasadena, CA 91107
Christopher.R.Wells@jpl.nasa.gov

Adam Zufall
NASA Ames Research Center
Freeman Ln
Mountain View, CA 94043
Adam.B.Zufall@nasa.gov

Paul A. Rosen
Jet Propulsion Laboratory
California Institute of Technology
4800 Oak Grove Dr.
Pasadena, CA 91107
Paul.A.Rosen@jpl.nasa.gov

***Abstract*—The National Academies of Science, Engineering and Medicine 2017 Decadal Survey of Earth Science and Applications identified geodetic measurements of surface deformation and related change as one of the top five "observables" to be prioritized in NASA's future program. In response, NASA commissioned a multi-center Surface Deformation and Change (SDC) team to perform a five year study of mission architectures that would support SDC observables and provide the most value to the diverse science and applications communities it serves. The study is being conducted in phases, in which the science and applications capabilities identified in the Decadal Survey are refined, candidate architectures and associated technologies to support these needs are identified, architectures are assessed against a science value framework specific to SDC, and recommendations to NASA are made. Ultimately, NASA will decide which amongst these recommendations will proceed to mission formulation. As synthetic aperture radar (SAR) was identified as the prime sensor technology to satisfy SDC observational needs, a key component of the SDC study is to assess the current state of the art in SAR sensor and supporting technology. The number of SAR systems, both civil and commercial, is growing rapidly, requiring that mission architectures not only consider technology, but availability of data from other missions, possible partnerships or collaborations, and even data purchase. The mechanism for assessment involves development of an end-to-end science performance evaluation tool for multi-satellite constellations, which feeds into a science value framework that considers science performance, technological programmatic risks, and cost. This paper will present an overview of the ongoing study including the candidate architectures and the technology road map needed to achieve the objectives of the mission.**

978-1-7281-7436-5/21/$31.00 ©2021 IEEE

TABLE OF CONTENTS

1. INTRODUCTION

The United States National Aeronautics and Space Administration (NASA) has initiated the Surface Deformation and Change Mission Architecture Study (SDC) in response to the needs of the United States research and applications community in the coming decades as expressed in the 2017 National Academies of Science, Engineering and Medicine Decadal Survey. SDC is one of a number of studies underway, each addressing different aspects of these needs. The SDC mission architecture is being formulated to acquire measurements of global changes in surface displacement and disruption down

2021 IEEE Aerospace Conference | 978-1-7281-7436-5/21/$31.00 ©2021 IEEE | DOI: 10.1109/AERO50100.2021.9438290

to the millimeter scale. The measurement also serves science communities interested in estimating global biomass and soil moisture, as well as applications such as emergency response to geohazards.

Origins of the SDC Mission Study

The National Research Council (NRC) assesses the needs for national investment in large civil space missions for NASA, NOAA, and USGS every ten years. The findings are released by the National Academies of Science, Engineering, and Medicine as Decadal Surveys [1]. The previous two surveys recommended synthetic aperture radar (SAR) missions for geophysical measurements of land surface. The 2007 survey recommendation has resulted in the NASA-ISRO SAR (NISAR) mission, which is nearing launch [2]. NISAR will measure surface deformation and land cover changes of all land and ice-covered surfaces using repeat-pass interferometric and polarimetric time-series measurements.

The 2017 Decadal Survey [3] recognized the need to continue these measurements beyond NISAR, with a particular emphasis on surface deformation and disruptive surface change, defining Surface Deformation and Change observables among its top priorities for the coming decade. However, rather than prescribing the mission including the instrument suite and concept of operations as was done in 2007, the 2017 survey prescribed only the observation without guidance on an underlying mission architecture.

In recent years, the orbital SAR landscape has changed considerably, with an expansion of national SAR programs around the world, and an increasing entrepreneurial interest in commercial SAR systems, data products and services. As these systems and services develop, their potential to fulfill SDC needs must be factored in. NASA has a long-standing policy to provide free and open access to data from its missions for both science and derived applications. For example, NISAR will deliver raw data, SAR imagery and derived interferometric and polarimetric products over all land and ice globally, sampled every 12 days from the ascending and descending parts of the orbit. Other agencies are also beginning to offer free and open data applicable to SDC observables.

To define a cost-effective, unique, and scientifically potent mission architecture in this complex civil and commercial playing field, NASA has commissioned mission studies in order to translate the SDC observables into a realizable mission implementation. Our group has been charged with systematically evaluating these options for SDC [4].

The 2017 decadal survey bounded the SDC mission study by providing the following guidance on the necessary observations:

- Measurement Technique: Interferometric repeat-pass SAR
- Temporal Sampling: Sub-weekly to daily
- Spatial Sampling: 5 to 15 m
- Vertical sensitivity: 1 to 10 mm
- Coverage: All land and coastal regions globally
- Mission Lifetime: 10+ years
- Maximum Phase A-F Cost: $ 500M

By not identifying any observable that mapped to a specific level of radiometric performance, the survey effectively opened the door for a "phase-only" mission architecture, where the radiometric quality of the image is too poor to be useful for imaging applications. However, NASA has directed the mission study to consider architectures that also provide useful imagery (noise equivalent $\sigma_0 < -20$ dB and ambiguities < -20 dB) [4]. NASA has a growing interest in commercial partnerships in Earth Science [5]: The SDC study considers commercial data-buy agreements and alternative space-segment acquisition strategies as part of the trade space to deliver the best value to NASA.

SAR Program of Record

The Decadal Survey recognized that SDC must be developed in the context of the "Program of Record," comprising systems and data sources that are expected to exist in the time frame when SDC would be operational, and that would provide suitable data for SDC-related research and applications. Access to SAR data for scientific applications is a key consideration in the Program of Record. Many of the science questions important to the SDC communities depend on global coverage with fine spatial resolution, weekly or sub-weekly temporal sampling, and long time series. Given these needs, commercially-priced or otherwise restricted data sets can greatly limit scientific productivity.

The availability of SAR data has been growing steadily over the past several decades [6], [7]. Through its long-standing free and open data policy, NASA has made SAR data available to the public since the 1980's, including those acquired through the NASA/JPL AIRSAR and UAVSAR airborne radar programs; SEASAT, flown in 1978; the shuttle imaging radar missions (SIR-A/B/C), flown in the 1980s; and the foundational digital topography produced by the Shuttle Radar Topography Mission in 2000. Other governmental entities are now adopting similar policies, for example the European Union's Copernicus program that includes the Sentinel-1 SAR constellation [8]. Sentinel-1 is currently the only operational SAR constellation with a free and open data policy, and will soon be joined by the NISAR and BIOMASS missions, which will greatly enhance the density of available measurements [9], [10].

Other missions that provide valuable but limited amounts of data to the Program of Record through Principal Investigator data grants include [11]: Japan's ALOS-2, Canada's RADARSAT-2, Italy's COSMO-SkyMed, Germany's TerraSAR-X and Tandem-X missions. Commercial arms of these missions also sell data. Commercial systems are also coming on line to supply SAR data to commercial markets, which could include scientists.

Future SAR missions with free and open data policies would extend this program of record. Some mission concepts currently being considered include the European Space Agency (ESA) ROSE-L mission [12], the German Space agency (DLR) Tandem-L [13], and of course SDC itself. These possible missions offer opportunities for collaboration in the pursuit of common goals. Other government and commercial-based systems could serve to augment the program of record through data purchases as long as that data could then become freely available after purchase.

Mission Study Organization

The Surface Deformation and Change mission study began in October 2018, as a five year project. The study comprises four phases:

1. Candidate Architectures (Oct. 2018 - Mar. 2021)
2. Assessment of Architectures (Mar. 2021 - Mar. 2022)
3. Architecture Design (Mar. 2022 - Mar. 2023)

4. Final Report and Selection (Mar. 2023 - Oct. 2023)

The initial phase of Candidate Architectures is the longest phase by design, to ensure evaluation of a wide range of architectures that arise when considering the many science needs, technological advances, international civil and commercial complementarity and possible partnerships. In this phase, the mission science and applications traceability matrix (SATM), trade space, and the driving capabilities are defined through modeling, research, and community feedback. Hundreds of concept designs are analyzed in terms of their performance and cost at a coarse scale, factoring cost and risk factors associated with new and emerging technological innovations in instrumentation, spacecraft, and constellation architectures. In the second phase, the promising architectures identified in Phase 1 will be studied in detail, resulting in refinements in our understanding of performance and cost as key inputs to a "science value" assessment, discussed in section 8. In Phase 3, we will reduce the trade space further to only a few architectures, which will undergo more detailed design and cost assessments, including greater emphasis on definition of data products, cal/val needs, and pre- and post-launch activities. Phase 4 is a reporting and transition phase, where the study team will summarize the top recommendations, NASA will decide how best to proceed, and in principle, the study will transition to formulation activities for the selected mission concept.

The SDC mission study is a team effort across NASA centers, with contributions from NASA Ames Research Center (ARC), Goddard Spaceflight Center (GSFC), Langley Research Center (LaRC), and Marshall Spaceflight Center (MSFC) under the lead of the Jet Propulsion Laboratory (JPL). Team members include scientists, engineers, and technologists, organized into smaller teams in the following areas: 1) architecture definition and evaluation; 2) technology assessment and development; 3) architecture performance tool development and performance assessment; 4) research and applications definition and community engagement; 5) value framework definition and application; and 6) commercial systems and data services assessment and engagement. In this paper, we describe progress to date and plans going forward in each of these areas.

The systematic process the architecture team has derived for defining and evaluating mission architectures is shown in Figure 1 with the remainder of the paper roughly organized into sections that feed into this process. After an initial brainstorming period that involves identifying desired capabilities and mission architecture classes that might deliver those capabilities, we go through an iterative process that considers a broad number of architectures at a very cursory level, to be followed by a narrowing of the candidate architectures and more detailed analysis on the remaining architectures during the second phase of the study. In each case, the criteria for selection or rejection is a cost-benefit analysis of the cost of the mission compared to the science value it delivers.

2. Candidate Mission Architectures

The process of identifying candidate mission architectures by starts with potential observation capabilities that have been identified from the science communities we serve. These capabilities can be either complementary or exclusive in relation to each other. From there, we have brainstormed broad architecture classes that might deliver such capabilities. These classes represent canonical representations of the concept of operations. Specific architectures that include such details as exact number of satellites, commercial data buy or international partnership possibilities, and observation plan follow by combining elements from the architecture classes to form a specific architecture concept of operations.

Observation Capabilities

The SDC observations are used in four science focus areas, which each have a number of observations, termed "geophysical observables", defined by the SATM. With a diverse set of observables under the SDC umbrella, there are many potential capabilities to consider. The following have been identified as the most critical set by the architecture team:

1. Continuity with the Program of Record
2. Decreasing temporal repeat times
3. Global spatial coverage capability
4. Error reduction by estimating tropospheric delay
5. 3D displacement vectors through look diversity

Sensor characteristics such as the frequency band, polarimetric diversity, and radiometric quality also factor into the capabilities of an observing system, and each capability has a unique impact on a potential SDC mission.

Continuity with the current program of record means that measurements from SDC can be used to add depth to the existing time series of interferograms. This record is expected to be present at a continuous 12 day interval globally once NISAR is operational but also includes the records obtained from other open access data such as Sentinel. In our SDC workshops, the science community has identified continuity as the top priority for SDC, while decreasing temporal repeat times is at the heart of the observations designated critical by the decadal survey. Meanwhile, orbital mechanics gives an inverse relationship between repeating ground track periods and the distance between adjacent ground tracks. Therefore, when combined with the capability for global spatial coverage, meaning all land and coastal regions for SDC, the challenge lies in increasing the coverage rate of the mission. There are fundamentally two options to increasing coverage rate once an observatory can operate continuously over all land: increase the swath width of a single spacecraft while maintaining performance or increase the number of satellites making the observation.

Another capability worth considering for SDC is to be able to make real-time estimates of the tropospheric delay. Though the troposphere makes up only 13 km of the path length of an orbital altitude many hundreds of kilometers, it contains 99% of all atmospheric water vapor by mass. Variations in the distribution of this water vapor alters the phase velocity of the radar signal, which manifests as errors in the phase measurement. The errors introduced by the tropospheric delay are the largest source of uncorrected error for NISAR. Though this issue would seem uncorrelated from the issue of temporal repeat times, there is a connection. NISAR addresses tropospheric error by averaging interferograms in the time-series to reduce the noise-like error source while pulling out the geodetic signal. This takes the 12-day sampling period to an effectively seasonal measurement of displacement. Having a real-time estimate of the tropospheric delay could eliminate the need for this averaging. Separating the tropospheric delay from the geodetic signal requires observing a common spot on the ground while traveling through separate paths in the atmosphere. This is achieved through either a bi-static measurement or multiple mono-static radar measurements.

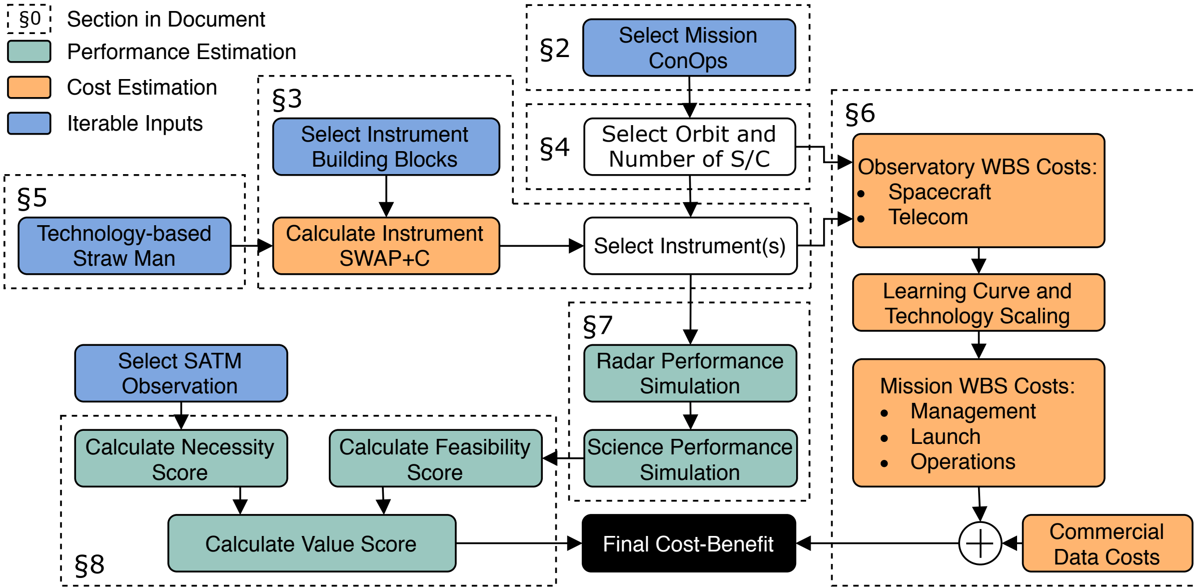

Figure 1: The SDC mission architecture evaluation process from a high level. The first phase of evaluation is designed to be a very rote process in order to quickly evaluate hundreds of potential architectures and identify key high level trends in architecture value.

Resolving the displacement vector accurately in all three spatial dimensions is a potential opportunity for new science over what is available on other orbital SAR systems. Individual interferograms are formed along their line of sight, which is typically at a slanted angle perpendicular to its velocity vector. NISAR observes all land and coastal regions both as it ascends in the orbit and also as it descends each orbit. The ascending and descending views provide a look diversity that enables the vertical component of deformation to be extracted, and can also give a good estimate of displacement in the East-West direction. However, because the orbit is near polar, estimates in the North-South direction are poor. Adding additional observations with more diverse lines of sight in the North-South direction would allow a complete spatial understanding of displacement. Such a capability could have profound impacts in certain science disciplines. Studies of ice rheology and basal friction that are dominated by shear flows would be greatly enhanced, as would the study of earthquake faults with predominantly longitudinal directions. Additionally, a full 3D displacement would allow translation of the displacement to any arbitrary direction. This means data from SDC could be translated into the line of sight direction for any SAR system and directly compared. Therefore, though this capability offers several attractive possibilities not included in the decadal survey it also ties in to data continuity, which is critically important to SDC's science community.

The previous measurement capabilities will have a strong influence on the number and configuration of satellites that would make up the SDC architecture. To these we also add the data product capabilities of frequency band, polarimetry, and radiometry. These capabilities will impact the data products that SDC would offer but they would not alter the orbital configuration of the space segment of the architecture. Frequency band plays a role in both foliage penetration (the ability to observe solid structure beneath the canopy of vegetation) and temporal decorrelation (the loss of phase coherence over time). For both of these factors longer wavelengths are preferred, however, longer wavelengths typically require larger and heavier hardware increasing cost. Polarimetry is the ability of the radar to measure the geometric orientation of the backscatter waves. Recent advances have combined polarimetry with interferometry using a technique called PolInSAR. Such capabilities add scientific value but also cost as additional channels of hardware are required and the antenna increases in complexity. Radiometry deals with the calibrated amplitude of a single SAR image. Though traditionally good radiometric imagery has been a prerequisite for forming interferograms, evidence suggests that the phase information from SAR backscatter can be preserved even in the presence of a lower signal to noise ratio to form quality interferograms. The attraction to sacrificing radiometric performance is cost savings as lowering the required signal to noise ratio would reduce the necessary size of the deployed antenna.

Note that many of the capabilities discussed in this section will involve a trade-off between observing swath and number of satellites, which combine to make up an overall coverage rate for the mission. A focus on smaller SAR observatories is therefore inevitable. It is important to highlight that SDC is not pursuing smaller payloads as a direct means to lower mission costs, but instead views smaller payloads as a means to enable unique capabilities and offer mission flexibility. To highlight this rationale, consider the cost curves in Figure 2, which shows instrument costs for various NASA radar instruments relative to NISAR costs. We created a straw man design for a smaller SAR system that was used for our first pass of evaluation. Please refer to section 3 for more information on the straw man creation process. This instrument utilized new technology advances to produce data products comparable to NISAR, but covers only one sixth of the swath. Utilizing the curve in Figure 2a and the estimated mass, we find that an individual smaller instrument should cost 70% less than NISAR. To achieve a similar coverage rate to NISAR, we would need to produce six of these identical smaller instruments. By producing multiple of the same product, we would expect to achieve some economies of scale. To model this, we used a learning curve with a 35% improvement factor, meaning the marginal cost per

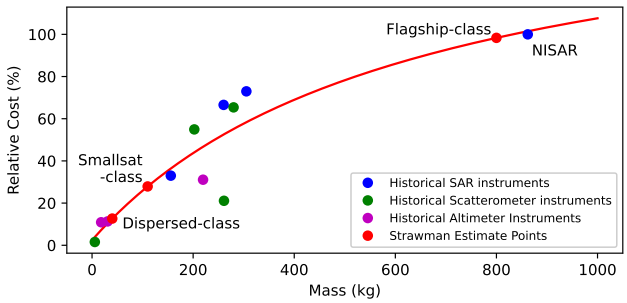

(a) Estimated instrument cost relative to mass using historical data from past NASA radar missions and normalized to the cost of NISAR. An investment in technology is expected to deliver necessary instrument performance at a lower mass point, thereby reducing instrument cost according to the curve.

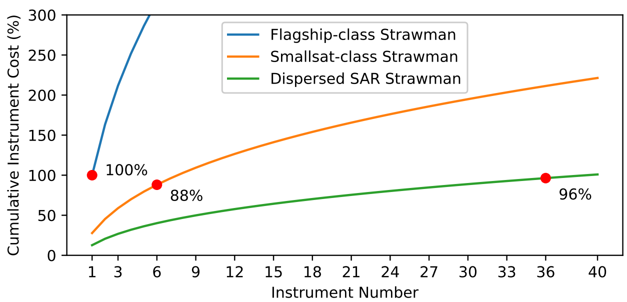

(b) Cumulative cost increase of all instruments as the number of identical instruments in the constellation increases. Costs are shown as a percentage of NISAR instrument costs. An improvement of 35% with every doubling of production quantity has been derived from past experience with smaller level unit builds.

Figure 2: A high level instrument cost analysis showing that sub-dividing the observation into multiple smaller instruments to achieve a constant coverage rate does not provide paradigm-altering cost savings. As such, the primary use of smaller platforms must be to deliver unique capabilities rather than cost savings.

unit decreases by 35% with each doubling of the production quantity. The cumulative cost of six satellites therefore comes to 88% of NISAR's cost. Further subdividing the instrument for a constant coverage rate shows similar trends. For example, dividing the six satellite sub-swaths into six additional sub-apertures for a dispersed SAR technique [14] produces 36 total satellites for the constellation. With a mass estimate of only 40 kg for these smaller satellites, the cumulative instrument cost for all 36 satellites comes to 96% of NISAR cost. With only a small cost savings projection for the increased risk, we have concluded that the use of smaller observatories must provide capability and flexibility rather than a means to provide significant cost savings, which will be relatively fixed for a desired coverage rate.

Mission Architecture Classes

The observation capabilities listed in the previous section lead to a number of mission architecture categories that SDC might consider. These architecture classes are not mutually exclusive, and elements from multiple classes may be combined to form unique architectures for evaluation. However, highlighting the distinct classes is useful as a demonstration of the techniques being considered for SDC. These architecture classes are broken down into six possibilities including: flagship-class observatories, sub-divided swath constellations, multi-squint formations, lowered inclination orbits, helical orbit formations, and passive co-flyers. Each of these classes offers a unique implementation approach in either the way it distributes satellites in the orbit, the way it handles observation swaths between adjacent ground tracks, or the number and variety of viewing angles it provides.

Flagship-class missions consist of satellites that cover the entire swath between adjacent ground tracks using a single instrument. These architectures are considered “flagships” because each satellite is self-sufficient at providing global coverage SAR data on its own. Improvements in coverage rate are achieved by adding observatories that are equally spaced around the orbit to provide denser time sampling under identical viewing geometries. In a multi-satellite constellation, the failure of a single satellite preserves global spatial coverage but reduces temporal sampling rate. This architecture has been the model for many of the current generation of orbital SAR constellations such as Cosmo-SkyMed and Sentinel-1 and as such has tended toward maximizing swath and minimizing orbit cycle time to use fewer satellites with greater capability. But a paradigm that optimizes the coverage rate with more satellites and adjusts the orbit repeat time and swath to fit is also possible. Because this architecture divides the constellation into self-sufficient elements, it is also well suited for international partnerships. SDC is actively involved in discussions with the international SAR community exploring ways to leverage common interests.

Another architecture technique is to have the swath between adjacent ground tracks equally sub-divided between multiple satellites. By placing these in the same orbital plane and controlling the sub-swath coverage via the spacecraft attitude, the aggregate group of constellations makes up the equivalent coverage rate of only a single flagship satellite. However, because the satellites are in the same orbital plane, they can be steered to cover the same sub-swath and would then provide faster interferometric repeats over that area. In this way, we can improve the repeat times for critical events while preserving a global coverage rate made up of smaller SAR satellites similar to that of NISAR. We expect this approach has the ability to deliver the capability of faster interferometric repeats for an architecture cost that does not exceed NISAR.

While the previous two architecture classes deal with adjusting the coverage rate of the mission architecture, they do not address other capabilities such as atmospheric error reduction and 3D displacement vectors. An architecture that would deliver both of these capabilities might fly three identical satellites in formation. The central satellite in the configuration flies using a standard zero-doppler geometry while satellites leading and lagging that satellite in the same orbital plane are squinted backward and forward respectively relative to the velocity vector at an angle of 10-15 degrees to all focus on the same region of ground. This configuration provides the look diversity to resolve the north-south shear displacements as well as multiple paths through the atmosphere to estimate the tropospheric delay component of the measurement. Dedicating three satellites to focus on a single swath instead of one would seem to have an adverse effect on the possible coverage rate of this architecture scheme. However, if the improved tropospheric estimate reduces the number of averages needed, a single 12-day repeat interferogram may be of equal quality to six two-day repeat interferograms averaged together without tropospheric removal.

A related architecture would fly a single SAR instrument at zero-doppler steering and have a passive co-flyer as its companion in formation. The passive instrument would receive the backscatter from the active instrument but the echo will take a different path through the troposphere, enabling the removal of that error source. However, this technique would not provide the independent looks necessary for three dimensional deformation estimates. The passive instrument would need to cover the same swath as the active instrument but by removing the active transmitter would have greatly reduced power draw and therefore is expected to provide a lower cost enhancement to the SAR data collection scheme employed.

The two remaining architecture schemes adjust the orbits used in order to seek synergies with science disciplines not related to repeat-pass interferometry. By creating a constellation using a lower inclination orbit, NASA could reduce non-interferometric revisit times over the lower latitudes to near daily times, which would be beneficial to science looking for fast time-series of SAR amplitude imagery. NASA would have to coordinate with an international partner or purchase data from a commercial provider for coverage of the polar regions. If used in coordination with another constellation with global monitoring, such as the proposed ROSE-L constellation, the look diversity provided by the lower inclination could provide 3D deformation estimation, though not tropospheric error removal because the measurements will not be simultaneous. Helical orbit formations are another alternate orbital configuration. Similar to the orbit of the TanDEM-X satellites, this configuration would provide a continuously changing spatial baseline for enabling interferometry beyond the repeat-pass interferometry observations prescribed by the decadal survey. Such a configuration with enough satellites would be enabling for the Surface Topography and Vegetation (STV) observable, a tomographic SAR measurement highlighted as an incubator in the decadal survey. Under the architecture concept for SDC, when not performing spatial interferometry or tomography, each satellite would cover adjacent swaths to form global repeat-pass observations similar to the sub-divided swath architecture.

The architecture configurations described here give canonical form to the variety of operational concepts under consideration for SDC. Specific architectures may mingle different aspects of these concepts in order to fully explore the cost and value trade space. When dealing with specific mission architectures, we have come up with a tag system to help keep the variety of options in perspective. The short-hand version of the tag has three characters: the band of the observing system, the total number of satellites comprising the mission, and a letter to uniquely capture all other elements. For example, an early architecture used for working through this process was an example of the sub-divided swath architecture using six satellites equally-spaced around the NISAR orbit to produce a potential for two-day repeat coverage over any 40 km swath. This architecture received the tag "L6A" because it was an L-band constellation utilizing 6 satellites and was the first architecture to do so. The next six satellite L-band architecture would receive the tag "L6B" and so forth. This naming system is important for being able to keep track of various permutations of the mission concepts presented here. Systematically optimizing that balance is the key work of the architecture study, and represents a new approach for major NASA Earth Science missions.

3. INSTRUMENT SELECTION

Once a candidate mission architecture concept is identified including the number of satellites and the coverage/capability scheme, an instrument must be selected to fill the required needs. This activity happens in conjunction with the orbit analysis described in the next section that optimizes the coverage rate of the architecture. To select the instrument, we have broken down the potential instrument capabilities into coarse discrete values. This approach sacrifices nuance to achieve a high level picture differentiating instruments for a given architecture. Shown in Table 1, these options make up the instrument trade space and the first building blocks for our analysis of cost and performance.

In order to systematically work through all possible instrument combinations from the trade space inputs shown in Table 1, the team put together an evaluation tool that would first estimate mass, power, and data rate of the instrument followed by its cost. The process starts by using the trade space inputs in the SAR signal to noise ratio equation to reverse out the necessary effective aperture size [15]. A "straw man" design is then chosen for a particular technology package, with a breakdown of mass and power estimates for each of the elements in the instrument. The straw man design has separate estimates for the instrument antenna and instrument electronics in order to allow mixing those technologies that are largely separable. When given as an input to the tool, the straw man design is then stretched and scaled according to the trade space inputs and derived antenna aperture to give mass and power estimates for a specific instrument. These mass and power estimates are then given to a modified version of the NASA Instrument Cost Model (NICM), which generates a cumulative instrument cost based on historical NASA instruments [16]. The resulting database output contains the resource usage including mass, power, data rate, aperture size, and cost for every possible combination from Table 1 that results in a physically realizable instrument. An example of the resulting instrument costs across several straw man technology packages is shown in Figure 3.

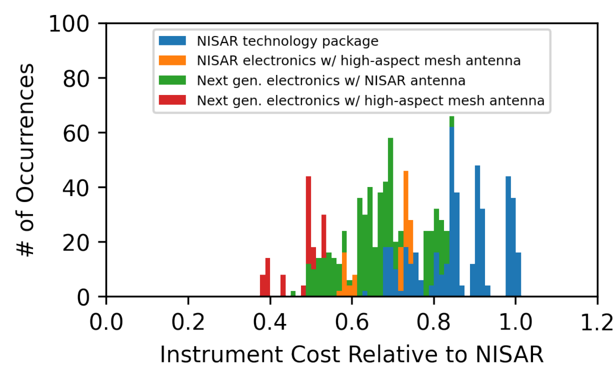

Figure 3: The instrument evaluation tool iterates over all possible combinations of Table 1 using the straw man input containing a particular set of technologies to produce instrument resource estimates including mass, power, and cost. Selecting the right instrument from this group depends on the concept of operations.

The first straw man design used for this process was the NISAR electronics and NISAR AstroMesh antenna using data that is readily available to the architecture team from the L-band NISAR instrument. If we are considering an instrument that calls for a SweepSAR instrument at S-

Instrument Capability	Option 1	Option 2	Option 3	Option 4	Option 5
Orbital Duty Cycle	15%	50%			
Scanning Mode	Passive	Stripmap	SweepSAR	ScanSAR	
Elevation Beamwidth	2 deg	3 deg	4 deg	6 deg	12 deg
Noise-Equivalent Signal Level	-15 dB	-25 dB			
Polarization Capability	Single-pol	Dual-pol	Quad-pol		
Frequency Band	X	C	S	L	
Single Look Resolution	15 m	10 m	5 m		

Table 1: Discrete breakdown of instrument capabilities being considered for SDC. Each combination of capabilities represents an instrument available for use in a mission architecture.

band frequency with only single-polarization capability and a beamwidth of six degrees rather than twelve, we must then scale the straw-man model accordingly. We do this by dropping the boxes required to form the second polarization, reducing the number of sweepSAR channels by half to account for the narrower swath coverage, scaling the mass proportional to the wavelength difference between L- and S-band, and scaling the supporting structural components to have the same ratio as using NISAR electronics. The result is not intended to replace a more detailed engineering effort, but rather to quickly evaluate thousands of different combinations in order to identify potentially promising architectures on which to focus those engineering resources.

We recognize that each straw man model has its limitations and analyzing the entire instrument trade space requires the use of several models. Rather than attempt to make each model fit the entire trade space where that may not be appropriate, we have enabled the evaluation tool to be able to identify conditions that are not well-suited to the model and reject them. For example, the NISAR straw man model is not well-suited to evaluating a ScanSAR instrument and therefore the tool does not evaluate those cases. Likewise the technologies and assumptions that go into the straw man model can have a significant impact on the mass, power, and cost results. Technology assessment and evaluation therefore plays a critical role in the mission architecture evaluation as discussed in section 5.

4. ORBIT SELECTION

The process of selecting the orbit for an SDC architecture begins with understanding the instruments that are included in the architecture definition. SDC architectures require a repeating ground-track orbit and are expected to achieve greater than 90% global coverage during the defined repeat cycle. The specification for the instrument beam width(s) combined with the allowable altitude range determines the length of the minimum repeat cycle that will enable the architecture to obtain the required global coverage. Once the orbit repeat cycle has been selected, the allowable altitude range is reduced to a few options.

With the orbit selection narrowed down to a small number of options, the flight dynamics team begins simulating the remaining candidates in STK. For each option, a satellite (or satellites) is placed into the candidate orbit and the full repeat cycle is modeled to determine instrument coverage capabilities. For configurations with multiple satellites, two variants are created so that the differences between formation flying and equally spaced configurations can be assessed. Multiple coverage and time between revisits metrics are computed after the simulation and the results are provided to the architecture team for review. After reviewing the specific performance of the orbit options, the architecture team selects the final orbit for the architecture.

Once the final orbit is selected, a SPICE SPK file is generated from the STK simulation for use by the Mission Planning and Performance Tool teams. This SPK file contains the orbit ephemeris for each of the spacecraft and allows these teams to directly import the satellite position information without needing to model the orbits within the Performance Tool software. To ensure appropriate documentation and traceability is maintained, the SPK file is archived within a team repository along with human readable metadata that defines the STK simulation setup and the summary products that were created to illustrate the coverage and revisit performance of the architecture.

5. TECHNOLOGY EVALUATION

The desired mission capabilities outlined in Section 2 focus on using multiple SAR satellite observations for either increased temporal sampling or look diversity. To be feasible in a cost-constrained environment, SDC must seek to minimize observatory outlays and maximize economies of scale. We have shown in Figure 2a that we expect investment in technology to impact our instrument cost estimate by reducing the mass and power of the instrument. This is a direct consequence of our modeling approach, based on the high-level NICM algorithm that takes these parameters as its only inputs. The SDC architecture study has therefore placed special emphasis on instrument component technologies that can deliver the elements of a SAR instrument with more efficient use of mass, power, or volume for a given performance level.

Our evaluation of technologies relevant to orbital SAR missions began with a technology workshop in May 2019 co-located with the Space Tech Expo in Pasadena, CA [17]. This venue allowed leadership and technologists within the study team to interact with a broad range of experts across several mission systems areas in a dialog between needs and current/future capabilities. The workshop helped solidify the study's approach to technology by stratifying SDC needs into three different tiers. Technologies that have cross-cutting application across the range of mission architectures being considered should receive our top consideration: most notably advances in integrated processing and thermal transport technologies. Technologies that are architecture-specific should also be considered, but the study team should first make key decisions about the nature of the mission architecture before seriously pursuing technology advancement. This category includes the critical, yet always custom antenna aperture for the instrument as well as aggressive technology goals such as sparse aperture instruments or robotic in-space assembly geared toward a specific architecture. Finally, many categories of mission systems such as launch vehicles, ground stations, and data distribution are being actively disrupted by a surge of commercial interest in Earth observation. These forces are larger than any single project can influence, and therefore SDC's approach will be to stay abreast of the latest developments in these areas and utilize advancements where applicable but not invest directly. These guiding principles have helped to shape the SDC technology road map discussed in the next section, but SDC's exploration of the technology landscape still continues. NASA has funded several technology surveys in critical areas in support of all the designated observable mission studies [18] running through the end of fiscal year 2021. SDC is an active participant in these studies and continues to seek out technology gaps that can help close the difference between desired capabilities and available funding.

Technology Road Map

Navigating the breadth of available technology innovations is difficult with the variety of potential mission architectures for SDC. However, the activity is a critical part of mission formulation within the project lifecycle as described in Table 2.2-1 and section 3.3 of the NASA System Engineering Handbook [19]. In order to deal with the complexity, and in keeping with the tiered technology strategy coming out of the technology workshop, SDC has organized a technology road map based on key architecture decisions. The road map places no time-constraints on development, but rather lists a variety of choices that should be made about the architecture before pursuing technology advancement in these areas. There are also several "off-ramps" that can adapt to more conservative or aggressive architecture concepts as the understanding of the mission evolves. Technology readiness assessment is one of the primary processes that will help to inform this decision and is discussed in the next section. Figure 4 shows a summarized version of this road map.

The first technologies to focus on are cross-cutting and would help reduce mass and volume for any instrument in any architecture being considered by SDC. The focus areas here are in multi-functional integration (shortened to "MF" in the figure) and thermal technologies. Multi-functional in this sense refers to the ability to combine many different behaviors into a single physical entity. For example, with the first early funding SDC has received we have explored the possibility of utilizing the high-speed transceivers on Xilinx Ultrascale FPGAs for direct RF generation of the radar waveform. If successful, placing this function within the DSP FPGA would eliminate the separate waveform generator and RF upconverter boxes used for NISAR, with the potential to save up to 40 kg of instrument mass if all supporting electronics can also be eliminated.

It is helpful to maximize the use of standardized interfaces, particularly in digital electronics, when seeking compact electronics solutions. The integrated ecosystems that are currently known to the team to be well-suited for multi-functional integration are SpaceVPX, CompactPCI, and a custom Common Instrument Electronics (CIE) ecosystem in development at JPL. CompactPCI is a longtime industry standard with significant fragmentation for specific designs, while SpaceVPX is a newer industry standard that attempts to standardize the PCI fragmentation while also expanding for the demands of the space environment. The CIE platform seeks even greater electronics density than the industry standards by eliminating many of the features unused in most NASA remote sensing instruments. The architecture team is considering all options in the architecture through the use of straw man designs as described in section 3. In terms of DSP technologies, SDC has identified that processing density can be improved by moving from the current space-qualified generation Virtex 5 to the next generation space-supported UltraScale devices. These add the aforementioned high-speed transceiver capability discussed previously. We also considered the terrestrial Ultrascale+ platform, which adds embedded digitizers directly to the FPGA chip and promises significant power savings. This technology received significant interest during our technology workshop, but subsequent data has indicated that potential radiation susceptibilities and lack of vendor support in the space environment would pose an unacceptable risk for a high priority decadal mission.

Thermal technologies are also enmeshed in the multi-functional integration focus. Thermal management is a key need in order to achieve orbital duty cycles of nearly 50% per orbit, and the reduction of volume introduced by advancing DSP technology increases the power density within the electronics, exacerbating the thermal problem. Fortunately, additive manufacturing has introduced revolutionary opportunities to combine structural and thermal elements within the same space. One technology that seems particularly promising is a passive two-phase heat pump that can increase thermal conductivity through a structure by a factor of 100 while requiring no external pumps that might add mass and reduce reliability [20].

Beyond the first cross-cutting technology focus, the architecture team must start to make decisions about the mission architecture in order to determine technology focus. The first decision regards antenna aperture characteristics. Active phased arrays have been traditionally used for SAR instruments and offer electronic steering flexibility that enables many operational capabilities. But NASA has recently eschewed this technology for SAR instruments in favor of large mesh reflectors that do not have active power electronics integrated. This technology achieves the lowest mass for the deployed aperture area, thereby lowering cost. SDC will have to re-evaluate the current state of both technologies in order to evaluate if the same dynamic still exists for the architecture concepts under evaluation. Beyond that, if the apertures are not large enough when deployed from smaller buses, more exotic deployment technologies such as robotic in-space assembly may be needed. If the architecture team then decides to pursue additional capabilities through increased look diversity, it will need to decide if independent or inter-dependent observatories offer the best value. In the case of inter-dependent observatories, we could then further subdivide the instrument observations to form a sparse aperture system. In an independent observatory scenario, the observations can either be divided among multiple spacecraft with combination on the ground, or through the use of a new type of instrument that can use differential absorption to estimate the water vapor content at the time of the measurement on the same spacecraft as the SAR instrument. These differential absorption radar (DAR) techniques have been demonstrated as profile measurements [21]. To be useful for SDC, innovations that would provide imaging at kilometer-scale resolutions would be needed. In all, the technology road map of Figure 4 provides a way to think about technology infusion necessary for the different architecture concepts for SDC and helps the team communicate priority and necessity of those technology

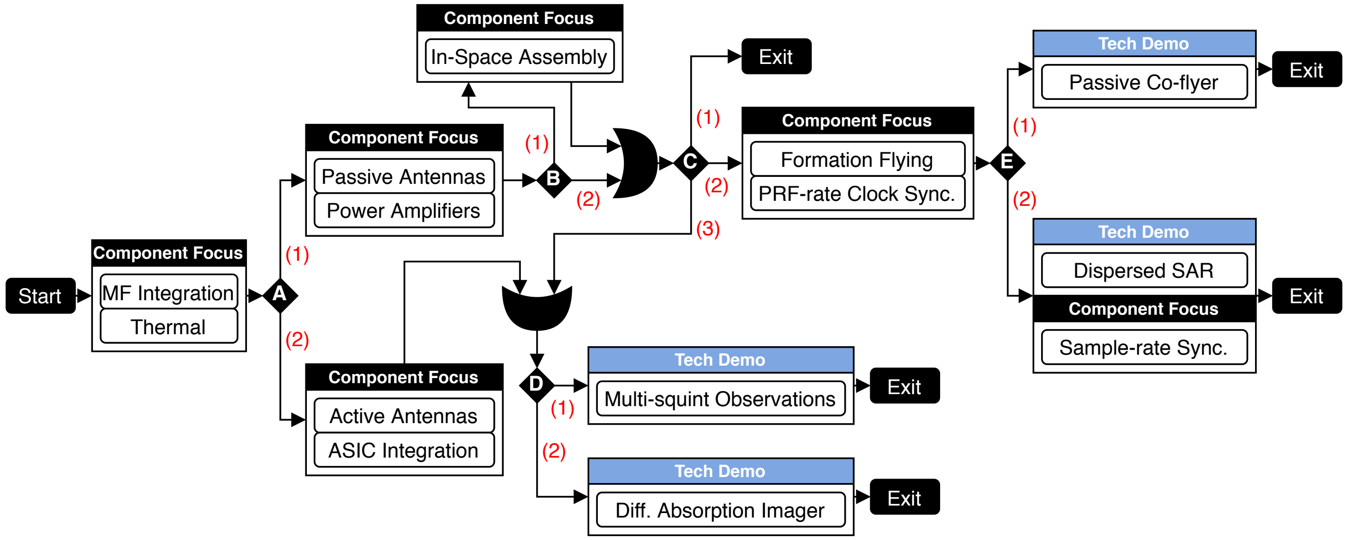

Decision Points:

A: (1) Focus on Stripmap/SweepSAR Instrument, (2) Focus on ScanSAR/TOPSAR Instrument
B: (1) Insufficient antenna aperture area for desired performance, (2) Sufficient performance with aperture area
C: (1) Pursue continuity mission, (2) Pursue Inter-dependent Observatories, (3) Pursue Independent Observatories
D: (1) Pursue multiple smaller spacecraft, (2) Pursue single spacecraft
E: (1) Pursue mother-ship augmentation, (2) Pursue distributed imaging capability

Figure 4: A high level version of the SDC technology road map that highlights key decision points throughout the architecture evaluation period.

gaps.

Technology Readiness Assessment

Technology readiness assessment (TRA) is the process by which technologies are evaluated for their maturity. NASA communicates this maturity through a technology readiness level (TRL) defined in Appendix E of NPR 7123.1 [22]. In 2014, NASA commissioned an evaluation of the TRA process that was completed with a number of recommendations in 2016 [23]. Two of the study contributors have produced a helpful paper defining an explicit process that follows these recommendations [24]. The SDC study team has adopted a specific implementation of this process for our own evaluation. The process involves answering a series of questions between the technologist and SDC as the customer that serve to define the scope of the technology in question as well as its current readiness level and potential risks to advancement.

These assessments serve several purposes within the architecture evaluation process. First, they provide a means to make more objective decisions to move down different branches of the technology road map in Figure 4. They also provide a clear means to scope proposal work for technology advancement. Finally, the results of this assessment are used in the mission cost estimation process to account for the technology advancement costs prior to PDR that are not captured otherwise. In the larger architecture evaluation process shown in Figure 1, this occurs in the step labeled "technology scaling", which we describe briefly below.

The instrument costs output by the NICM model in section 3 are based on costs from phase B to D in the NASA project lifecycle, which occur after technology development should be complete. To account for this cost gap, we must estimate the additional costs in pre-phase A and phase A for technology advancement needed for a given instrument.

The technology assessment process evaluates only specific technologies rather than the instrument as a whole. We must therefore perform an instrument-level TRA that packages all of the technologies incorporated in that instrument. From that assessment we calculate a scaling term from a curve based on Figure 10 in Malone *et al.* [25]. That scaling term is applied to the NICM output to append the estimated cost of technology advancement for the instrument. Note that for situations where the instrument is assessed at higher than TRL 6, for example a mission that re-builds a significant portion of the NISAR L-band instrument, the scaling curve provides a small discount over the stated NICM value.

6. Mission Cost Evaluation

The mission cost evaluation process consists of making estimates across different mission systems areas as specified by the NASA work breakdown structure (WBS) [26]. At the current estimation fidelity we are only operating at the second level of the WBS, but by structuring our estimates according to this structure early, we can easily refine estimates by diving deeper into the hierarchy during the evaluation period of the study.

Mission WBS categories are broken into broad systems categories such as integration and test, launch, operations, and ground data. The instrument and spacecraft make two additional line items in the WBS that have been estimated from the previous sections. The traditional NASA WBS is setup to handle a single spacecraft with multiple instruments. SDC is considering many different constellation configurations. Most include multiple identical spacecraft and instruments, a few include two different types of spacecraft each with different instruments. The SDC WBS will eventually need to be setup to distinguish recurring costs like manufacturing from non-recurring costs like design at levels immediately below the instrument. Also, since instrument and spacecraft operate at the same WBS level, it is difficult to identify which instruments might belong to one of multiple spacecraft. Despite these potential future pitfalls, which we expect to encounter during the phase two evaluation, we have not altered the traditional WBS structure at this stage.

SDC makes direct estimates of spacecraft bus, launch vehicle, and telecom costs for preliminary estimation. We are able to do this based on high level instrument resource estimates of mass, power, data rate, and deployed aperture area. Other elements in the WBS are estimated as a percentage of either the instrument cost, spacecraft cost, or the observatory cost made up of the combined spacecraft and instrument.

Spacecraft Bus Cost Estimation

The spacecraft bus comprises all of the spacecraft mission systems needed to operate the spacecraft and communicate with the ground. Today many spacecraft bus configurations are available commercial-off-the-shelf (COTS) in a preconfigured package that would suit most end users. Unfortunately, SAR instruments typically strain the use cases for such buses. Most prominently, the large aperture required for the measurement will require larger reaction wheel systems for pointing control than are typically offered in a COTS package. But the large power draw or high data rate may also be limiting factors. An intriguing question from our initial technology workshop will be explored during the evaluation period: whether it would be more cost-effective to purchase an over-specified COTS bus, for example more power and mass capability then needed in order to support reaction wheels for a large cantilevered antenna, or custom build a smaller spacecraft tailored to the exact instrument needs.

For our initial cost estimates, SDC is making tiered spacecraft cost estimates based on the mass, power, and aperture size of the instrument. The estimate is not specific to any particular bus vendor or offering but intended to capture a mean cost for spacecraft in that particular class. Recall that the purpose of these first pass estimates is to be able to compare many tens or hundreds of architectures quickly, while the effort in phase two of the study is to refine these estimates after promising architectures have been identified. Pairing instruments with candidate buses including estimates for all of the bus subsystems will be a key part of phase two activities and involve concurrent engineering teams at multiple NASA centers.

Our estimation levels for phase one therefore fall into one of four categories of buses: small, medium, large, and flagship. Small spacecraft buses support instrument payloads up to 350 kg with 1300 W of peak payload power. Medium buses support 450 kg payloads, while large buses support 1000 kg payloads. Flagship buses are larger than typical COTS offerings and would need to be custom-built, this applies for anything over the large bus limits.

Launch Cost Estimation

Launch costs are estimated in a similar manner to spacecraft buses. Using the combined observatory mass and expected stowed volume, we make estimates of cost for a given class of payload capacity. These estimates are not based on any particular vendor or offering but rather on an average value at that class using current launch prices from the LSP catalog. Launch tiers are broken down into similar levels as spacecraft buses with small, medium, large, and flagship designations. Each corresponds closely to the mass ratings of the spacecraft bus, but may jump a level depending on the additional mass or volume of the instrument.

Telecom Cost Estimation

SAR observing systems produce large amounts of raw data, and the SDC science community would like to get all of it to the ground to maximize the potential for ground-breaking research. As such, the spacecraft will most likely require a custom data handling system (DHS) to manage the overall spacecraft activity. This includes maintaining timing, interpreting commands from the ground, collection, processing, and formatting of the telemetry data to be down-linked, and high-level fault management and safing routines. Additionally, the spacecraft requires a large capacity recorder to store the raw radar data and support high-speed data transfers. The spacecraft communications design includes a telecommunications system designed to communicate with ground stations that command and control the spacecraft, as well as accommodate down linking and processing the large amounts of raw science data. The quality of science measurements improve with increased number of observations, therefore the spacecraft down links require a high bandwidth with sufficient view periods of ground stations.

The DHS also includes a spacecraft radio system to facilitate data exchange with the mission ground system via a network of ground stations. Up-linked data supports command and control of the spacecraft, while engineering and raw instrument science data (high volume) are sent in a downlink stream. The quality of science measurements improve with increased number of observations and resolution and the resulting data volume is proportional. Data volume combined with latency are the two mission requirements that drive telecommunication system design. The down-link bandwidth, and the length and frequency of radio contacts are the primary factors that establish sufficient communications to support mission drivers. These three parameters provide the primary trade space for the mission telecommunications architecture study.

NISAR, the predecessor mission, largely establishes the nominal mission data volume. The mission also provides one possible telecommunication system architecture which acts as a "reference" for comparison to an optimized telecommunication system architecture.

The flow of the telecommunication architecture study will be as follows. We will first confirm the driving mission requirements. We will then perform a technology search to establish telecommunication architecture system options. The search assumes no major development costs by SDC directly, but rather expects to follow the industry technology trends that develop over the SDC development period. It will assure broad reach across NASA, commercial missions and manufactures. We will also investigate network options and spacecraft transceiver options. For each mission architecture option we must develop scenario-specific requirements before developing telecommunication system options for each. The resulting output will be a cost estimate and estimate of the size, weight, and power of the telecom system needed for SDC.

To date the study has confirmed the driving requirements similar to the NISAR mission are pertinent. However, latency is of more interest for the SDC study. For technology, the viability of the NASA ground and space based networks well into the 2030s was confirmed by the study. The study also determined that there are multiple commercial radio networks being developed that could likely support SDC using standard radio protocols. The study has suggested that a high performance optical solution is developing; but will depend heavily on external funding to mature. Finally, the study has developed an options template that was used to document telecommunication options for one particular SDC architecture being studied.

Scaling Identical Observatories

Many of the architectures under consideration for SDC use multiple identical observatories to make up the complete observing system. It is reasonable to expect that there are certain recurring costs that would make the production of identical hardware progressively cheaper as more units are built with some diminishing returns. One of the findings from our technology workshop was that many of the industry experts in attendance agreed with this sentiment and from their experience the expected gains followed a mathematical learning curve [17].

The learning curve function is also known as the cumulative average model and was first expressed from observations in the aircraft industry [27]. It gives the cost, C, of an Nth unit of production as:

$$C = aN^b \tag{1}$$

where a is the cost of a single unit, and b is a rate of improvement. The rate of improvement can be thought of as a percentage that describes the cost reduction for every doubling of production quantity. For SDC, we have used an improvement rate of 35% derived from our own experience on moderate sized production levels of smaller flight electronics builds. In the evaluation process of Figure 1, this cost scaling term is being applied to the entire observatory cost estimate. The cumulative sum of these costs has been shown in Figure 2b as part of our demonstration highlighting that these economies of scale will not significantly lower the cost of a fixed coverage rate for SAR observations.

7. Science Performance Model

The SDC Science Performance Model (SPM) consists of a set of tools that calculate spatially-varying measurement uncertainties for a given set of point target locations on the surface of the Earth. Currently, the SPM is capable of calculating errors for observations of surface deformation and biomass, using estimated errors in radar phase and backscatter, respectively. In order to produce spatially-varying uncertainties for different surface targets, the model takes into account instrument parameters and orbital calculations combined with a mission plan, information about global conditions of the Earth's surface (e.g., terrain type, snow and vegetation cover, topography), and time-dependent models that represent propagation delays through the troposphere and ionosphere. The tool combines all the aforementioned information to calculate seasonal error statistics for a set of targets, which can then be combined into long-term performance estimates for a given architecture.

Different architectures will be evaluated through the SPM as described below. We use the "L6A" architecture described in section 2 to explain different parts of SPM including its inputs and outputs. This architecture uses 6 satellites with 2° elevation beamwidth (as opposed to 12° for NISAR). All the satellites are distributed uniformly in the NISAR orbit having a 12 day repeat time. Therefore, each satellite individually has 12-days between interferometric observations but leads/lags two days from its neighbors. In an urgent response situation, each one of the satellites mechanically adjusts its attitude to cover the same region, making a 2-day interferometric repeat over a single 40 km swath.

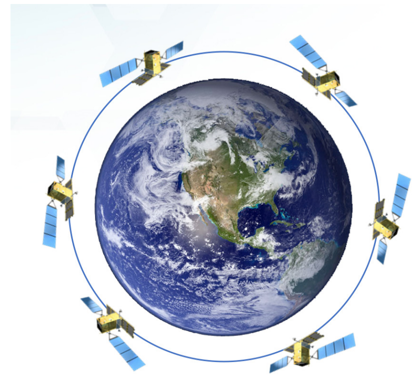

Figure 5: The schematic configuration of 6 Satellites in NISAR orbit with 2 days separation

Figure 5 shows the orbital configuration of architecture L6A discussed in section 2. The six satellites in L6A are distributed evenly in the NISAR orbit with 2 days separation between their ground tracks. The next subsection discusses different inputs to SPM and some specific inputs for L6A configuration, followed by a subsection on the output of SPM as applied to the L6A example.

Inputs to the SPM

In order to estimate the accuracy of deformation and biomass measurements for a particular architecture, the SPM must take into account the major error sources that limit the accuracy of SAR and InSAR observations. The model includes a number of possible error sources. The dominant errors are related to seasonally-dependent global models of ionospheric and tropospheric propagation delays, as well as the effects of interferometric decorrelation. To account for these error sources, several global databases are used as input in the NISAR performance modeling tool. The databases used in SPM include: 1. ionospheric spatial spectra, 2. temporal decorrelation map, 3. radar backscatter map, 4. biomass map, 5. elevation and slope map, 6. terrain class map, 7. percentage vegetation cover map, 8. snow cover map, 9. tropospheric spatial spectra, 10. cryosphere velocity, 11. cryosphere classification. In addition to the detailed radar instrument model and mission plan files, the NISAR performance tool attempts to account for environmental factors when estimating radar backscatter and interferometric phase uncertainties.

Temporal correlation and ionospheric delay models were designed for L-band measurements, and need to be modified so that they can be applied to a variety of architectures operating at different frequencies. To generate global temporal coherence and backscatter maps using Sentinel-1 data at C-band, a commercial vendor has been selected to perform this task through evaluating the responses to an RFP.

Ionosphere Model Error—The model currently used to estimate ionospheric phase delays in the SPM was inherited from the NISAR Performance Tool, and is based on a combination of empirical measurements from the L-Band ALOS sensor and the WBMOD Ionospheric Scintillation Model. It was precisely tailored to apply to the calculation of ionospheric delays specific to the NISAR wavelength, observation geometry, and orbital timing. However, the architectures under consideration in the SDC study are not restricted to L-band systems, and may also differ from NISAR in terms of look geometries and mission plans, causing differences in the expected ionospheric phase propagation errors. In order to accommodate a more flexible trade space, we are in the process of developing a new ionospheric model based on total electron content (TEC) measurements obtained empirically from Global Navigation Satellite System (GNSS) data.

Ionospheric small-scale and large-scale total electron content (TEC) gradients in both latitude and longitude directions can be measured in TEC units per kilometer (TECU/km) using Global Navigation Satellite System (GNSS) data [28]. The small-scale TEC gradients (SSTGs) are derived from measurements of vertical TEC differences with spacings ranging approximately from 2 km to 12 km at 350 km altitude. The large-scale TEC gradients (LSTGs) are computed from global TEC maps that are generated with TEC data distributed at spatial scales of hundreds of kilometers. To characterize various ionospheric conditions, statistics such as mean, root-mean-square, and standard deviation of SSTG measurements can be obtained for local areas with a number of data samples from tracking multiple GNSS satellites. Regional and global maps of a combination of the SSTG statistics and LSTGs can also be obtained as snapshots using data from networks of tens to thousands of ground-based GNSS receivers global TEC maps. These TEC gradient data can be used to measure ionospheric-induced delay and phase variations in azimuth and range directions of spaceborne synthetic aperture radar data. The SSTGs can also be used to measure ionospheric irregularities that cause ionospheric scintillation in radar signals.

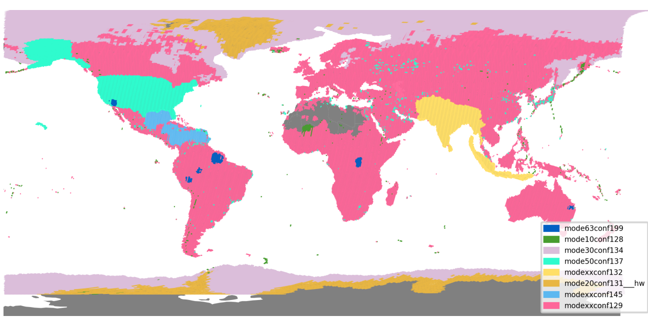

Figure 6: Output CLASP coverage map on a 12-day horizon, descending node only, one color per instrument mode, for the L6A scenario

Mission Plan— Observation plans are produced with the Compressed Large-scale Activity Scheduling and Planning (CLASP) tool, an artificial intelligence mission planner software currently being developed for the NISAR mission [29] and already used operationally for scheduling imaging by two instruments on-board the International Space Station: the ECOSTRESS instrument [30] and the Orbiting Carbon Observatory-3 [31]. CLASP is a long-range scheduler for space-based or aerial instruments that can be modelled as pushbrooms – 1-dimension line sensors dragged across the surface of the body being observed. It addresses the problem of choosing the orientation (in case steering is possible) and on/off times of a pushbroom instrument or collection of pushbroom instruments such that the schedule covers as many target points as possible, without oversubscribing memory and energy. Orientation and time of observation is derived from geometric computations that CLASP performs using the SPICE ephemeris toolkit [32]. A thorough description of the combinatorial so-called *coverage* problem as well as algorithms to solve it are described in [33].

Inputs of CLASP notably include (1) campaign files describing desired geographical areas to be observed along with required instrument mode and geometric and temporal constraints. Each campaign is assigned a priority which determines the order in which resources (steering capability, energy, memory) will be allocated to it; (2) constellation definition which can be made of one or several spacecraft, each of which has one or several body-mounted instruments with specific *swaths* modeled as pushbroom sensors. Geometry of the sensors are parameterized by minimum and maximum look angles as angles rotated about the velocity vector of the spacecraft from the nadir look vector, looking 90 degrees off of velocity. Energy on-board each spacecraft is modelled as a timeline resource which is depleted at a specified rate for each instrument mode when an observation is being done and augmented constantly with the production of solar panels, taking eclipses into account. Constraints ensure that the energy level never falls below a minimum and that a specified handover state is achieved at the end of each revisit period.

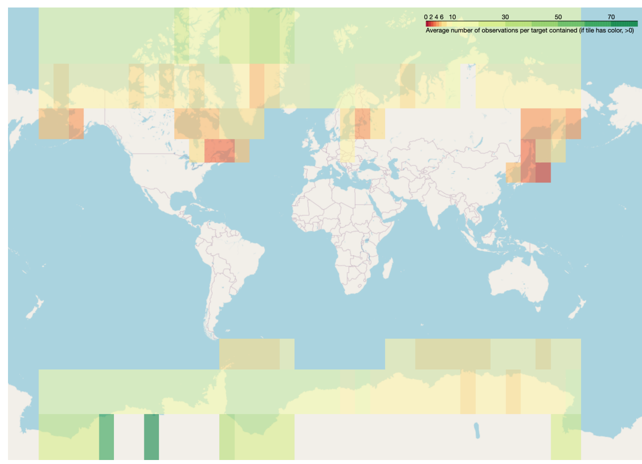

(a) Single-pol coverage heat map

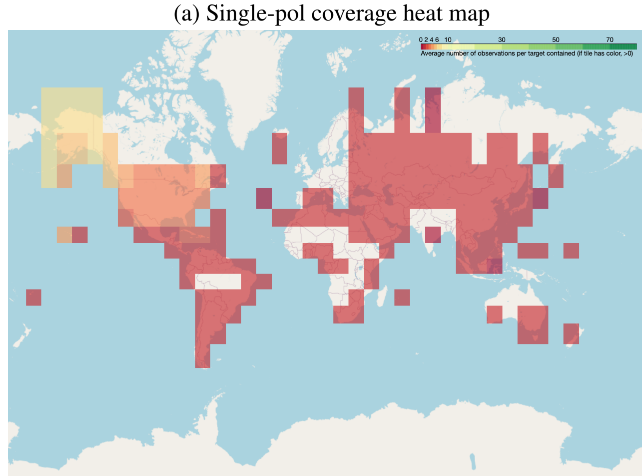

(b) Dual-pol coverage heat map

Figure 7: Coverage heat maps for two instrument modes on a 12-day horizon for the L6A scenario. Color of each 5°×5°tile depicts the average number of observations per target in the area (shown tiles are above 0° and below 80° latitude).

CLASP outputs one schedule per spacecraft as a list of timed observations with their corresponding geographic coordinates and steering angles. Several types of charts can also be consulted, such as a coverage map (see Figure 6) primarily showing with what instrument mode a zone has been observed, coverage heatmaps showing the number of times a zone has been observed in a specific instrument mode (see Figure 7), or other charts related to the state of the spacecraft (e.g. memory usage or power levels).

Instrument Simulation— SPM uses some characteristics of the radar instrument to calculate the error in biomass or deformation estimation models [34]. The radar instrument characteristics used in SPM include:

1. Range bandwidth 2. Antenna azimuth dimension 3. Beamwidths 4. Null-to-3-dB relationships 5. Total ambiguities 6. Range/azimuth weighting factor 7. Number of bits in ADC 8. Noise equivalent σ^0

For the L6A configuration, we use SAUSAGE, a JPL SAR performance simulation tool, to calculate the radar characteristics for 48 different modes. Different modes are identified based on their ground range resolution and polarization as defined in the instrument trade space shown in Table 1, and starting look angles of 30, 32, 34, 36, 38, and 40 degrees as required from the concept of operations. SPM uses the SAUSAGE outputs for each of these modes to extract all the required characteristics mentioned above.

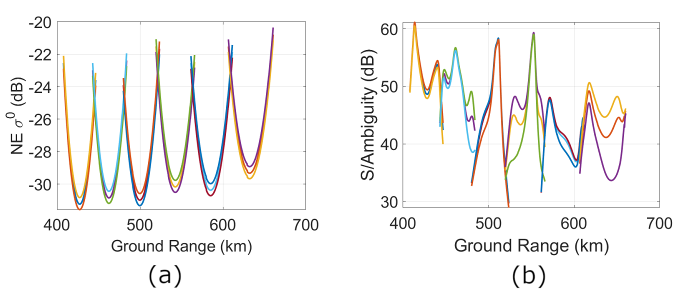

Figure 8: (a) Noise Equivalent σ^0 (b) Signal to Ambiguity, of the instrument at HH polarization for dual-pol system. Curves from near range to far range in both (a) and (b) correspond to look angles 30,32, 34, 36, 38, and 40 degrees, respectively. Different colors are for resolutions 5, 10, and 15m. The 5m resolution has lowest S/Ambiguity and highest Noise Equivalent σ^0.

Figure 8 (a) and (b) show the Noise equivalent σ^0 and Signal to Ambiguity ratio, respectively. These plots are for HH polarization of a dual-polarization system. Different colors correspond to different single-look resolutions of 5, 10, and 15 meters. Each set of curves from near range to far range in both (a) and (b) correspond to the look angles specified previously. Therefore, each group of three different color curves in these figures corresponds to a specific look angle. The 5 m resolution has the highest noise equivalent σ^0 at any specific look angle in Figure 8 (a). This is due to the fact that the higher resolution mode has larger bandwidth. Therefore, the received noise power is larger. The signal to ambiguity ratio at 5 m resolution is lowest of any specific look angle in Figure 8 (b). These outputs from the instrument performance simulation become inputs to SPM to evaluate the performance of the data products.

SPM Error Models

To quantify the errors for any geophysical observable for a given architecture through SPM, we need a global map of all the locations relevant to that specific geophysical observable, such as biomass or solid earth. We also need an error model relating the geophysical observable error to the measurement error. In this section, we explain the biomass and deformation error models, respectively.

Biomass Error Model— Estimating the amount of above ground biomass in forested areas is critical to develop a better understanding of ecosystem processes. There have been a wide variety of studies conducted over the past three decades showing how radar polarimetric measurements can be used to estimate above ground carbon for regions with less than 100 Mg of biomass per hectare. A biomass error model is used in SPM to assess the biomass estimation accuracy over biomass target map. The SPM calculates the implications of this error model on the performance of a polarimetric radar using instrument, mission, and science parameters from the inputs explained previously [34]. Using the first-order Taylor's expansion of biomass b as a function of backscatter parameters, $(\sigma_{hh} \quad \sigma_{hv} \quad \sigma_{vv})$, and compensating for having correlated noise between the various components we can write biomass estimation error as:

$$\Delta^2 b = \left[\frac{\partial b}{\partial \sigma_{hh}} \Delta\sigma_{hh} \quad \frac{\partial b}{\partial \sigma_{hv}} \Delta\sigma_{hv} \quad \frac{\partial b}{\partial \sigma_{vv}} \Delta\sigma_{vv} \right] \times \Gamma \times \begin{bmatrix} \frac{\partial b}{\partial \sigma_{hh}} \Delta\sigma_{hh} \\ \frac{\partial b}{\partial \sigma_{hv}} \Delta\sigma_{hv} \\ \frac{\partial b}{\partial \sigma_{vv}} \Delta\sigma_{vv} \end{bmatrix} \tag{2}$$

where Γ is the correlation matrix of polarimetric measurements to biomass. The SPM uses the inputs given to calculate the variance of backscattered power measurements, $(\Delta\sigma_{hh} \quad \Delta\sigma_{hv} \quad \Delta\sigma_{vv})$ due to different error sources such as SNR, calibration error, and area projection error [34]. A semi-empirical model is developed to relate the polarimetric backscatter measurements to biomass. Using this model, we can calculate the derivative of biomass with respect to backscattered power [34]. The resulting outputs from these models will be discussed after introducing the deformation model.

*Deformation Model—*Interferometric measurements of deformation in the line of sight (LOS) of the satellite can be related to the radar phase using the following equation:

$$\phi = \frac{4\pi}{\lambda} \Delta\rho \tag{3}$$

where ϕ is the phase, λ is the radar wavelength, and $\Delta\rho$ is the ground displacement between two InSAR acquisitions. This equation assumes that the satellite's perpendicular baseline is zero, or that the topographic contribution to the range change has been perfectly corrected.

The interferometric phase error, defined as any component of the InSAR phase that does not correspond to displacement, consists of multiple components: decorrelation, tropospheric delay, ionospheric noise, and random errors attributed to processing artifacts, as shown in the equation below:

$$\Sigma_{total} = \Sigma_{decor} + \Sigma_{tropo} + \Sigma_{iono} + \Sigma_{proc} \qquad (4)$$

Each of the components, except for the processing errors, are provided as a globally-varying input layer to SPM, calculated from empirical measurements or published error models. An example of this is the method for estimating the ionospheric contribution discussed previously. In addition to evaluating the error in LOS displacements, SPM is capable of estimating vector deformation error in the North, East, and vertical directions, given an observation with a minimum of 3 distinct satellite look geometries. This functionality is necessary for evaluating the three dimensional displacement capability discussed in section 2.

SPM Outputs

SPM is a tool that simulates observations made by the different mission architectures identified in the trade space study, and estimates the measurement accuracy of geophysical observables (deformation, biomass, and disturbance detection). By comparing the performance of each architecture against the desired capabilities for different applications outlined in the Science and Application Traceability Matrix (SATM), we aim to evaluate a given architecture's science performance, contributing to its overall value. SPM generates error maps for biomass and deformation models. However, other science and applications can be integrated into SPM if the error model and target map are provided.

Performance Map— Using the inputs and error models described previously, SPM calculates the science error estimation for all the targets for that science discipline. We show examples of error maps for biomass and deformation below. These maps will be used to generate a feasibility score for a specific architecture, as described in section 8.

Biomass—As mentioned in the discussion of the biomass error model, SPM calculates the biomass error due to different error sources. We use L6A architecture as an example here to demonstrate the biomass error outputs. Figure 9a shows the total number of observation per biomass target in one year for this architecture. As seen in this figure, the number of observations increases as the target gets further from the equator. This is due to the overlap between different passes. On the other hand, we see a large number of observations in Alaska compared to targets with the same latitude. This is due to a high priority being assigned to a campaign covering Alaska and requesting of as many observations as possible for that region. Figure 9b shows the biomass error (Mg/ha) for all biomass targets with biomass less than 100 (Mg/ha). We only show error maps less than 20%.

The performance maps of Figure 9b show regional nuance in biomass estimation that will be important for detailed architecture study, but a summary statistic is also needed for broad architecture comparisons. The biomass model uses the ratio of all biomass targets with biomass error less than 20 Mg/ha as its summary statistic. For the L6A architecture shown in the figure, this number is equal to 94%. The SPM will also calculate the revisit rate for this measurement. These two estimates must be compared with the desired SATM performance characteristics to come up with a single feasibility score for the architecture as discussed in section 8.

Deformation— The primary output of the SPM deformation error model consists of seasonal heat maps that show expected deformation errors for a particular set of ground targets relevant to a given geophysical observable. Figure 10 shows expected LOS measurement errors for ground targets relevant to studies of geohazards for the L6A example architecture. The seasonal deformation error maps generated by SPM are shown in Figure 10 and can be condensed to generate summary statistics for a geophysical observable, showing the feasibility of measuring that observable with a particular architecture. First, statistics are calculated for each season in terms of coverage and displacement error. The coverage is expressed as a percentage of the targets where observations are possible for each season, and the displacement error is shown in millimeters for one interferogram. We show an example of seasonal statistics for the L6A architecture in Table 2.

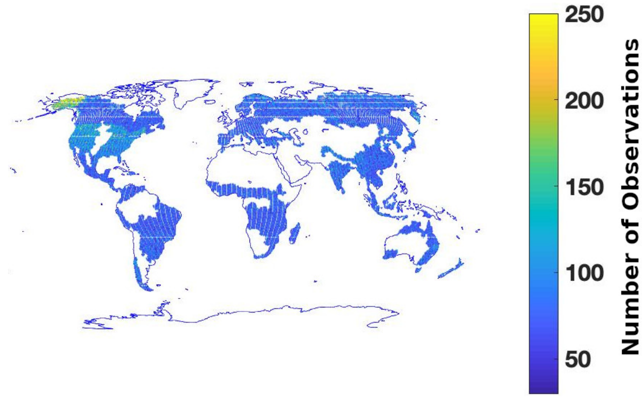

(a) The total number of observation in one year over simulated targets.

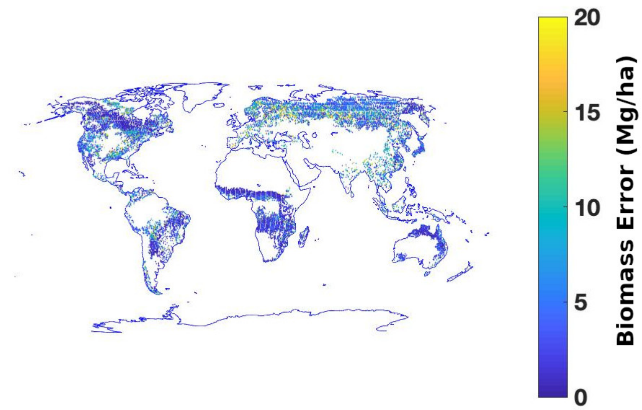

(b) Biomass error estimation for configuration (2)

Figure 9: Geolocated outputs from the SPM provide regional detail about architecture performance.

Category	Coverage	DU (mm)
Winter	74.6%	10.0
Spring	80.9%	10.1
Summer	96.1%	13.2
Fall	94.2%	9.1

Table 2: Example seasonal statistics output by the performance tool for the geohazards target set, with "DU" meaning displacement uncertainty.

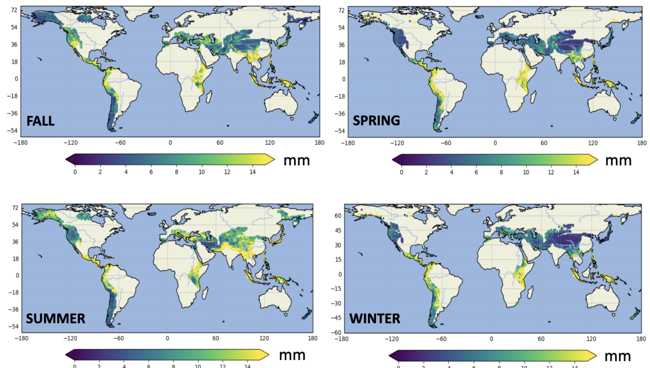

Figure 10: For deformation estimates, the SPM captures seasonal variation in science performance caused by snow coverage and precession of the Earth.

The seasonal statistics can be further generalized into overall (i.e., average) coverage and error estimates for the geophysical observable. An example is shown in Table 3 for the geohazards target set. A target set is used in SPM to to represent the regions of interest for an analysis. Multiple geophysical observables can use the same target set, in this case all geohazards observables would use the target set shown. The values in the table then say that 83.1% of the targets have better than 9.2 mm uncertainty over a specified spatial scale. SPM also computes the number of valid interferometric pairs generated over a season. By preserving SPM outputs, we expect to be able to use these summary statistics as a jumping off point to dive back into the more detailed performance maps to provide nuance for architecture performance comparison.

Category	**Coverage**	**DU (mm)**
Geohazards	83.1%	9.2

Table 3: Example summary statistics for the geohazards target set, with "DU" meaning displacement uncertainty. The performance tool has a separate target set for each science focus area.

8. VALUE FRAMEWORK

After the set of candidate observing system architectures is identified, a process for comparing and assessing the candidates is necessary. Within the SDC architecture study this process is referred to as the value framework. The value framework will need to provide a mechanism for discriminating between architectures that is traceable to the Decadal Survey objectives as defined in the SATM and allows for a transparent process for down-selection within the candidate architecture trade space. The framework will need to assess each architecture in multiple dimensions, including Science and Applications performance, responsiveness to the Decadal Survey, mission and programmatic risk factors, affordability, and schedule.

As part of the value framework, Measures of Effectiveness (MOEs) will be established to quantify the science and applications benefit enabled by each candidate architecture under consideration. Currently two MOEs are envisioned for evaluation of science and applications performance. These have been termed "necessity" to indicate the value of a particular observable to its science objective, and "feasibility" to indicate how well a particular architecture meets these needs.

Necessity Score

A necessity score will be assigned to each geophysical observable for each science and applications objective identified in the SATM. This score will be used to describe how important a geophysical observable is in satisfying the associated objective. One implementation under consideration would require the sum of all necessity scores associated with a given objective to be constrained to sum to 1.0. For example, a notional objective which has two equally important geophysical observables associated with it would have each geophysical observable be assigned a score of 0.5. Alternatively, if one observable is twice as important as the other, than the more critical observable would be assigned a score of 0.67 and the less important observable would be assigned a score of 0.33. Note that the necessity score as envisioned is not dependent on the candidate architectures being considered and is instead derived from the science and applications objectives by the members of the research and applications focus area to which the observable belongs.

Feasibility Score

To incorporate the specifics of the candidate architectures, a separate MOE will be necessary, and will be referred to as a feasibility score. Similar to the necessity score, the feasibility score is assigned at the geophysical observable level. The score will describe the capability of a given candidate architecture to make the measurement of the geophysical observable as specified in the SATM. Unlike the necessity score however, the feasibility scores for geophysical observables associated with a science and applications objective are not coupled and can be assigned independently. A candidate observing system architecture which is capable of measuring a geophysical observable as specified in the SATM would receive a feasibility score between 0.0 and 1.0 for that particular geophysical observable, whereas a candidate that is incapable of measuring a geophysical observable at all would receive a score of 0.0. Determination of the feasibility score will leverage performance estimates generated by the SPM when available and will consider parameters such as frequency bands, polarization, spatial resolution, revisit time, data latency, accuracy, and coverage.

Some observables in the SATM do not have performance models in the SPM for evaluation. The biomass and deformation models cover the majority of our primary observable objectives, but there are several observables such as snow-water equivalent and surface water extent for which we do not presently have calibrated science performance models. Feasibility scores must find a way to keep scoring consistent between these different levels of fidelity, which makes it likely that a tiered approach will be selected for these scores. In such a system, higher fidelity SPM estimates will be compared against a set of thresholds from the SATM to assign the feasibility score, while observables without models will have more qualitative estimates compared to similar threshold derivations. The exact score levels must be finalized by the start of our phase two evaluations in April.

Final Value Score

After the necessity and feasibility scores are assigned, they can be used to quantify the science and applications benefit of a given candidate observing system architecture within the context of the SDC SATM and the Decadal Survey. Multiple options for utilizing these MOEs are under consideration by the SDC architecture study team, including options which would use relative weighting of the science and applications objectives. We should note that the final science and applications value score is not the only term used to accept or reject an architecture. The score is a summarized representation of the architecture's science and applications performance in numeric form, but does not take into account factors such as affordability, schedule, and risk. The final value score will need to be weighed against these other programmatic factors before an observing system architecture recommendation can be provided to NASA Earth Science Division.

9. SUMMARY

The mission architecture studies for the Earth Science decadal survey represent a new approach to the traditional NASA designated mission by separating the desired observable from the mission design. The architecture study team is specifically tasked with taking a rigorous and systematic approach to the evaluation of mission implementations in order to assess the costs and benefits they provide. The process put together for the Surface Deformation and Change observable applies this approach to repeat-pass interferometric SAR, an area with growing commercial and international interest. We are now two years into our five year study and have identified the processes we will use for evaluation as well as 33 candidate architectures for consideration. These candidates range in capability from traditional single spacecraft to various techniques using constellations of smaller satellites to provide targeted increases in coverage rate, either through decreased repeat time or increased look diversity. As we proceed into the evaluation phase of our study we will use the processes described here to score as well as start to narrow the possibilities and work toward a final mission architecture recommendation to the NASA Earth Science Division for the SDC observation.

ACKNOWLEDGMENTS

The research was carried out at the Jet Propulsion Laboratory, California Institute of Technology, under a contract with the National Aeronautics and Space Administration (80NM0018D0004). The authors thank the NASA Earth Science Division of the Science Mission Directorate for funding and overseeing this effort including Gerald Bawden, Mitra Dutta, Charles Webb, Sandra Cauffman, and Karen St. Germain. The authors would also like to thank Shanti Rao, Vianni Ricano-Cadenas, Jim Dempsey, Katherine McBrayer, and Josh Doubleday for their contributions to this effort.

REFERENCES

[1] S. S. Board, N. R. Council *et al.*, *Earth science and applications from space: urgent needs and opportunities to serve the nation*. National Academies Press, 2005.

[2] ——, *Earth science and applications from space: national imperatives for the next decade and beyond*. National Academies Press, 2007.

[3] S. S. Board, N. A. of Sciences *et al.*, *Thriving on our changing planet: A decadal strategy for Earth observation from space*. National Academies Press, 2019.

[4] P. A. Rosen, S. J. Horst, A. Khazendar, P. Milillo, S. Oveisgharan, S. E. Owen, B. Osmanoglu, J. Sauber-Rosenberg, A. Molthan, K. Case *et al.*, "Nasa's next generation surface deformation and change observing system architecture," in *IGARSS 2019-2019 IEEE International Geoscience and Remote Sensing Symposium*. IEEE, 2019, pp. 8378–8380.

[5] J. Favors, S. Cauffman, J. A. Kaye, E. Ianson, L. Friedl, W. W. Turner, K. Gaddis, K. J. Murphy, A. Whitehurst, D. S. Green *et al.*, "Nasa earth science partnerships-lessons learned in measuring, managing, and maturing public-private partnerships in the earth sciences," *AGUFM*, vol. 2019, pp. PA54B–03, 2019.

[6] A. Moreira, "A golden age for spaceborne sar systems," in *2014 20th International Conference on Microwaves, Radar and Wireless Communications (MIKON)*. IEEE, 2014, pp. 1–4.

[7] P. A. Rosen, "The renaissance in radar remote sensing: our new vision for earth and the planets," in *EUSAR 2017; 11th European Conference on Synthetic Aperture Radar*. VDE, 2017.

[8] P. Breger, "The copernicus full, free and open data policy," 2017.

[9] P. A. Rosen and R. Kumar, "The nisar mission–an nasa/isro space partnership supporting global research and applications," in *2019 URSI Asia-Pacific Radio Science Conference (AP-RASC)*. IEEE, 2019, pp. 1–1.

[10] S. Quegan, T. Le Toan, J. Chave, J. Dall, J.-F. Exbrayat, D. H. T. Minh, M. Lomas, M. M. D'Alessandro, P. Paillou, K. Papathanassiou *et al.*, "The european space agency biomass mission: Measuring forest above-ground biomass from space," *Remote Sensing of Environment*, vol. 227, pp. 44–60, 2019.

[11] F. Meyer, "Spaceborne synthetic aperture radar: Principles, data access, and basic processing techniques," *Synthetic Aperture Radar (SAR) Handbook: Comprehensive Methodologies for Forest Monitoring and Biomass Estimation*, pp. 21–64, 2019.

[12] N. Pierdicca, M. Davidson, M. Chini, W. Dierking, S. Djavidnia, J. Haarpaintner, G. Hajduch, G. V. Laurin, M. Lavalle, C. López-Martínez *et al.*, "The copernicus l-band sar mission rose-l (radar observing system for europe)(conference presentation)," in *Active and Passive Microwave Remote Sensing for Environmental Monitoring III*, vol. 11154. International Society for Optics and Photonics, 2019, p. 111540E.

[13] D. Schulze, C. Wecklich, M. Bachmann, R. Kahle, and M. Wermuth, "The operations concept for tandem-l–from mission goals to spacecraft requirements," *70th International Astronautical Congress (IAC)*, 2019.

[14] J. Mittermayer, P. Lopez-Dekker, T. Kraus, and G. Krieger, "Small Satellite Dispersed SAR - an Exemplary Configuration," in *Proceedings of EUSAR 2016: 11th European Conference on Synthetic Aperture Radar*, Jun. 2016, pp. 1–4.

[15] J. C. Curlander and R. N. McDonough, *Synthetic Aperture Radar: Systems and Signal Processing*, 1st ed. Wiley-Interscience, Nov. 1991.

[16] J. Mrozinski, H. Habib-Agahi, G. Fox, and G. G. Ball, "Latest NASA Instrument Cost Model (NICM) Version VI," in *AIAA SPACE 2014 Conference and Exposition*. American Institute of Aeronautics and Astronautics, 2014, _eprint: https://arc.aiaa.org/doi/pdf/10.2514/6.2014-

4205. [Online]. Available: https://arc.aiaa.org/doi/abs/10.2514/6.2014-4205

[17] SDC Technology Steering Committee, “Surface Deformation and Change Technology Survey,” NASA, Tech. Rep., May 2019. [Online]. Available: https://science.nasa.gov/earth-science/decadal-sdc

[18] K. St. Germain, “Earth Science Division Decadal Survey Briefing with Stakeholders,” Jul. 2020. [Online]. Available: https://science.nasa.gov/science-red/s3fs-public/atoms/files/ESD-DS-Community-Forum-July-16-2020-FINAL.pdf

[19] G. Shea, “NASA Systems Engineering Handbook Revision 2,” Jun. 2017. [Online]. Available: http://www.nasa.gov/connect/ebooks/nasa-systems-engineering-handbook

[20] E. Sunada, P. Bhandari, B. Carroll, T. Hendricks, B. Furst, J. Kempenaar, G. Birur, H. Nagai, T. Daimaru, K. Sakamoto, S. Cappucci, and J. Mizerak, “A Two-Phase Mechanically Pumped Fluid Loop for Thermal Control of Deep Space Science Missions,” in *46th International Conference on Environmental Systems*, Vienna, Austria, Jul. 2016.

[21] L. Millán, R. Roy, and M. Lebsock, “Assessment of global total column water vapor sounding using a spaceborne differential absorption radar,” *Atmospheric Measurement Techniques*, vol. 13, no. 10, pp. 5193–5205, Oct. 2020, publisher: Copernicus GmbH. [Online]. Available: https://amt.copernicus.org/articles/13/5193/2020/

[22] Office of the Chief Engineer, “NASA Systems Engineering Processes and Requirements,” NASA, NASA Procedural Requirements NPR 7123.1C, Feb. 2020. [Online]. Available: https://nodis3.gsfc.nasa.gov/

[23] S. Hirshorn and S. Jeffries, “Final Report of the NASA Technology Readiness Assessment (TRA) Study Team,” NASA, Tech. Rep. HQ-E-DAA-TN43005, Mar. 2016. [Online]. Available: https://ntrs.nasa.gov/citations/20170005794

[24] M. A. Frerking and P. M. Beauchamp, “JPL technology readiness assessment guideline,” in *2016 IEEE Aerospace Conference*, Mar. 2016, pp. 1–10.

[25] P. Malone, R. Smoker, H. Apgar, and L. Wolfarth, “The application of trl metrics to existing cost prediction models,” in *2011 Aerospace Conference*, March 2011, pp. 1–12.

[26] S. Terrell, “NASA Work Breakdown Structure (WBS) Handbook,” NASA, Tech. Rep. HQ-E-DAA-TN51989, Jan. 2018. [Online]. Available: https://ntrs.nasa.gov/citations/20180000844

[27] T. P. Wright, “Factors Affecting the Cost of Airplanes,” *Journal of the Aeronautical Sciences*, vol. 3, no. 4, pp. 122–128, 1936. [Online]. Available: https://doi.org/10.2514/8.155

[28] X. Pi, S. Oveisgharan, E. Tymofyeyeva, H. Fattahi, and P. Rosen, “Measuring ionospheric tec gradients and irregularities from ground-based gnss observations,” in *Proc. ION ITM*, 2021.

[29] J. R. Doubleday, “Three petabytes or bust: Planning science observations for nisar,” in *SPIE 9881*, New Delhi, India, May 2016.

[30] A. Yelamanchili, S. Chien, A. Moy, E. Shao, M. Trowbridge, K. Cawse-Nicholson, J. Padams, and D. Freeborn, “Automated science scheduling for the ecostress mission,” in *International Workshop for Planning and Scheduling for Space (IWPSS 2019)*, Berkeley, California, USA, July 2019, pp. 204–211, also appears at ICAPS SPARK 2019.

[31] A. Moy, A. Yelamanchili, S. Chien, A. Eldering, and R. Pavlick, “Automated scheduling for the oco-3 mission,” in *International Workshop for Planning and Scheduling for Space (IWPSS 2019)*, Berkeley, California, USA, July 2019, pp. 195–203.

[32] C. H. Acton, “Ancillary data services of nasa’s navigation and ancillary information facility,” *Planetary and Space Science*, vol. 44, no. 1, pp. 65 – 70, 1996, planetary data system.

[33] A. Maillard, S. Chien, and C. Wells, “Coverage planning under geometric constraints,” *AIAA Journal of Aerospace Information Systems*, accepted, 2020.

[34] S. Hensley, S. Oveisgharan, S. Saatchi, M. Simard, R. Ahmed, and Z. Haddad, “An Error Model for Biomass Estimates Derived From Polarimetric Radar Backscatter,” *IEEE Transactions on Geoscience and Remote Sensing*, vol. 52, no. 7, pp. 4065–4082, 2014.

BIOGRAPHY

Stephen Horst *holds Ph.D. and M.S. degrees in Electrical Engineering from Georgia Institute of Technology, and a B.S. in Electrical Engineering from The Ohio State University. He is currently serving as the architecture and technology lead for phase I of the SDC mission architecture study. He has spent the past ten years at the Jet Propulsion Laboratory working on technology and engineering for repeat-pass interferometry using synthetic aperture radar via the NISAR mission and is familiar with the thermal challenges facing such systems as the lead designer for the NISAR transmit/receive modules. Dr. Horst is a 2020 NASA Honor Award recipient for applying radar electronics technologies to NASA future mission concepts.*

Jonathan Chrone *is an Aerospace Engineer at NASA Langley Research Center (LaRC) in the Systems Analysis and Concepts. He has supported numerous NASA Earth Science missions since 2005 and currently serves as the Science Team lead for the LaRC Space Missions Analysis Branch.*

Shaun Deacon *Shaun Deacon received his B.S. and M.S. degrees in Aerospace Engineering from Embry-Riddle Aeronautical University in 2005 and 2008 respectively and has supported the Space Mission Analysis Branch at NASA Langley Research Center since June 2008. In that time, he has supported mission design activities within multiple Langley flight projects and has contributed to a range of early concept development activities within Langley’s Engineering and Science Directorates.*

Charles T-C Le *received the Ph.D. degree from the University of Washington, Seattle, WA in 1996. He has been with the Jet Propulsion Laboratory since 1996, and is currently a Signal Analysis Engineer within the Radar Algorithms and Processing Group of the Radar Section. His research interests include electromagnetic scatting theory, and various aspects in active and passive microwave remote sensing, such as technology development, algorithm design, system modeling and simulation, and instrument implementation, integration, and test.*

Adrien Maillard *holds a Dipl. Ing. from INSA Toulouse (France) and a Ph.D. in Computer Science from ISAE-SUPAERO (France). He is a Postdoctoral Associate in the Artificial Intelligence Group at the Jet Propulsion laboratory. His interests focus on artificial intelligence planning and scheduling for space systems.*

Andrew Molthan *is the Deputy Branch Chief for Earth Science at NASA Marshall Spaceflight Center. He is a co-lead of the research and applications team for the ongoing SDC Decadal Survey/Designated Observables Studyhelping to broaden research and applications for various architectures proposed by the study plan participants.*

Anh N. Nguyen *is a Small Satellite Specialist, and holds a B.Sc. in Computer Engineering and a Ph.D. in Aerospace Engineering with focus in precision guidance, navigation, and control of drag-free small spacecraft for Earth Geodesy applications. Her expertise at NASA Ames Research Center are the development and execution of small satellite mission architectures.*

Batuhan Osmanoglu *, Research Physical Scientist, holds a B.Sc. in telecommunications engineering and a Ph.D. in synthetic aperture radar (SAR) interferometry. He has been a part of Istanbul Technical University, University of Miami, University of Alaska Fairbanks developing his primary area of expertise in radar remote sensing, and has worked on applications for observing surface deformation, measuring target velocities, and radar design. Since 2013 he has been working at the NASA Goddard Space Flight Center. He is working on instrument and algorithm development of P-, L-, X- and Ku-band SAR systems. He also serves as one of the NISAR Deputy Application Leads at NASA, and is one of the Disasters Program coordinators at Goddard. He is a member of the IEEE and American Geophysical Union. He also chairs the Microwave Remote Sensing workgroup under International Society for Photogrammetry and Remote-Sensing.*

Shadi Oveisgharan *was born in Isfahan, Iran. She received the B.Sc. degree from the Sharif University of Technology, Tehran, and the M.S. degree from the University of Michigan, Ann Arbor, MI, both in electrical engineering, and the Ph.D. degree in electrical engineering from Stanford University, Stanford, CA. She is currently serving as the science performance tool lead for phase I of the SDC mission. She awarded NASA Postdoctoral Program (NPP) in 2007. She joined JPL as a Scientist in 2010 and was involved in many different projects and missions including NISAR and SMAP missions. Her current research interests include InSAR radar remote sensing and modeling electromagnetic scattering in snow and vegetation.*

Martin Perrine *is a Scientist/Faculty Specialist at the University of Maryland's Earth System Science Interdisciplinary Center (ESSIC), where he performs science radar development, operations and data analysis for NASA/Goddard Space Flight Center's science mission. Prior to joining ESSIC he was an Electrical Engineer at three Federal agencies including NASA where he supported radio system development. He also worked on the regulation of radio systems for the Federal Communication Commission and developed radio systems for the Department of Defense. He received an M.S.E.E. from Johns Hopkins University in 1987 and a B.S.E.E from Michigan State University, 1984.*

Rashmi Shah *(S'06, M'14, SM' 17) received B.S. in Electrical Engineering in 2007 from Rochester Institute of Technology. She then got her M.S. and Ph.D. in Aeronautical and Astronautical Engineering from Purdue University, West Lafayette, IN, USA, in 2010 and 2014, respectively. Since 2014, she has been at Jet Propulsion Laboratory (JPL), California Institute of Technology (Caltech), Pasadena, CA, USA as a research technologist in the Tracking Systems and Applications Section. Her background and interests are microwave remote sensing technology development and remote sensing using signals of opportunity reflectometry. She is also part of the core team member for JPL Foundry's A-team where she works with teams on early concept development. Dr. Shah is the recipient of NASA Early Career Public Achievement Medal and Institute of Electrical and Electronics Engineers (IEEE) Geoscience and Remote Sensing Society's (GRSS) Early Career Award. She is a senior member of IEEE. She serves as a co-chair of GNSS and Signals of Opportunity Working Group for the IEEE GRSS Society's Instrumentation and Future Technologies Technical Committee. She also serves as a chapter chair for IEEE Metropolitan Los Angeles GRSS Chapter.*

Ekaterina Tymofyeyeva *received her B.S. degree in physics from The College of New Jersey in 2009, and a Ph.D. in earth science from the University of California, San Diego in 2018. Her research interests include using Interferometric Synthetic Aperture Radar (InSAR) and Global Positioning System (GPS) measurements of crustal deformation to further the understanding of the earthquake cycle. Dr. Tymofyeyeva is currently working with the NASA-ISRO Synthetic Aperture Radar (NISAR) Algorithm Development Team at the Jet Propulsion Laboratory (JPL), California Institute of Technology (CalTech) in Pasadena. She is also serving as a Deputy Program Applications Co-lead for the NISAR mission, and an acting member of the WinSAR Executive Committee.*

Christopher Wells *holds a B.A. in Computer Science from the State University of New York at Oswego. He is currently a Data Scientist in the Artificial Intelligence Group at the Jet Propulsion Laboratory.*

Adam Zufall *is an ADCS engineer at the NASA Ames Research Center, holds a M.Sc. in Astronautics from Stanford University, and is a PhD Candidate at UC Davis. He has been part of several CubeSat development teams at Ames, spanning the life cycle from initial concept, design, integration, and mission operations. His research centers on applying high-performance attitude systems on low-power hardware and on quick-turn missions.*

Paul A. Rosen *(S/'78, M/'03, SM/'05, F/'10) received a PhD in Electrical Engineering from Stanford University and his M.S. and B.S in Electrical Engineering from University of Pennsylvania. He is currently Project Scientist for NASA-ISRO synthetic aperture radar mission (NISAR) at the Jet Propulsion Laboratory, California Institute of Technology (Caltech). He is also the study coordinator for NASA's Surface Deformation and Change Decadal Survey Architecture Study. His assignments at JPL have encompassed scientific and engineering research and development of radar instruments and applications, as well as technical, organizational and programmatic management of radar developments at JPL. Dr. Rosen is a visiting faculty member at the Division of Geological and Planetary Sciences at Caltech, and has authored on over 40 journal and book chapter publications, and over 100 conference papers. He currently serves as the IEEE Geoscience and Remote Sensing Society Director for Global Activities.*